Polymer 51 (2010) 2112–2118

Contents lists available at ScienceDirect

Polymer

journal homepage: www.elsevier.com/locate/polymer

Cyclic poly(dimethylsiloxane) from kinetically controlled cyclodepolymerization of linear precursors in dilute solution

Marcus Foston, Haskell W. Beckham*

School of Polymer, Textile and Fiber Engineering, Georgia Institute of Technology, Atlanta, GA 30332-0295, USA

ARTICLE INFO

Article history:
Received 6 December 2009
Received in revised form
24 February 2010
Accepted 24 February 2010
Available online 4 March 2010

Keywords:
Cyclic poly(dimethylsiloxane)
Dual-detector GPC
Monte Carlo simulation

ABSTRACT

Cyclic poly(dimethylsiloxane) (PDMS), $[(CH_3)_2SiO]_x$ or D_x, was prepared in high yield (>70% for $x > 12$) from commercially available linear α,ω-dihydroxy-PDMS by base-catalyzed unimolecular ring closure in dilute solution. Cyclization, which occurs with formation of charged linear byproducts, was confirmed by GPC, FTIR, MALDI-ToF and NMR spectroscopy. Product mixtures were analyzed with a newly developed dual-detector GPC method in which the linear byproducts were end-labeled with a UV-absorbing group and separately detectable with a UV detector. Alternatively, charged linear byproducts were removed with anion-exchange resin. Yields and molecular weight distributions of the cyclic products are consistent with Monte Carlo simulations of kinetically controlled cyclodepolymerization. Large cycles from this cyclodepolymerization route are obtained in much higher yields (>70% for $x > 12$) than those reported for the traditional base-catalyzed ring-chain equilibration of D_4 and D_5 (~13% for $x > 6$) [1].

1. Introduction

Cyclic dimethylsiloxanes (D_x) have been prepared traditionally by acid- or base-catalyzed ring-chain equilibration of $[(CH_3)_2SiO]_x$ ($x = 3$, 4 or 5) in the bulk or in solution [2–4]. After refluxing for several days, this method produces an equilibrate composed mostly of cyclic material, $[(CH_3)_2SiO]_x$, in which the ring concentration of a given size decreases in a mostly continuous fashion with increasing molecular weight. Exhaustive purification of these mixtures using distillation, fractionation and preparative gel permeation chromatography [1,5] are successful in isolating narrow fractions of cyclic PDMS up to molecular weights of 50 kg/mol (~1300 ring atoms). However, yields for any given cycle size are rather limited. For example, Dodgson and Semlyen reported that the base-catalyzed equilibration of $[(CH_3)_2SiO]_4$ and $[(CH_3)_2SiO]_5$ in toluene took several days and resulted in approximately 13% yield for all large ($x > 6$) cyclic siloxanes [1].

High yield synthesis of cyclic PDMS may be achieved by ring closure of end-functionalized linear PDMS using a complementary difunctional coupling agent in dilute solution [6]. This end coupling dilute solution route was demonstrated on commercially available α,ω-dihydroxy-PDMS (M_n ~ 2.5 kg/mol), which was converted to cyclic PDMS in 77% yield. This published method begins with deprotonation of the α,ω-dihydroxy-PDMS precursor with sodium hydride followed by stirring overnight or until all solid particulates dissolve. After addition of a dichlorodimethylsilane coupling agent, the reaction was allowed to proceed for another 24 h before quenching with an anion-exchange resin to remove any remaining charged linear species. The product was washed with water to remove salts and vacuum distilled to remove low-molecular weight byproducts. The cyclic architecture of the PDMS product was proven by MALDI-ToF mass spectrometry, GPC, IR and NMR spectroscopy.

In this synthetic procedure, α,ω-dihydroxy-PDMS is deprotonated in dilute solution for some time before the coupling agent is added. During this time, a number of reactions can take place as shown in Fig. 1. Of particular interest here is the formation of cyclic PDMS by depolymerization of linear PDMS. Depolymerization of high-molecular weight linear polymers to form cyclic oligomers, often but not always in dilute solution, is referred to as cyclodepolymerization. All polymers prepared by step-growth methods may by cyclodepolymerized, as demonstrated already for a very large variety of polyesters [7–9], polyamides [10], high-performance aromatic polymers [10,11], and olefin-containing polymers [12]. Catalysts must be employed and range from simple bases [13] to Grubb's catalyst [12] to enzymes [7]. The goals of these cyclodepolymerization studies include the preparation of cyclic oligomers that can be used as (a) starting materials in entropically-driven ring opening polymerizations, (b) hosts for guest binding, and (c) components for multicyclic macromolecules such as polyrotaxanes [14,15]. It has also been suggested that cyclodepolymerization and entropically-driven ring-opening polymerization can be used as an interesting route for the material recycling of polymers [16].

* Corresponding author. Tel.: +1 404 894 4198; fax: +1 404 894 7452.
E-mail address: beckham@gatech.edu (H.W. Beckham).

0032-3861/$ – see front matter © 2010 Elsevier Ltd. All rights reserved.
doi:10.1016/j.polymer.2010.02.043

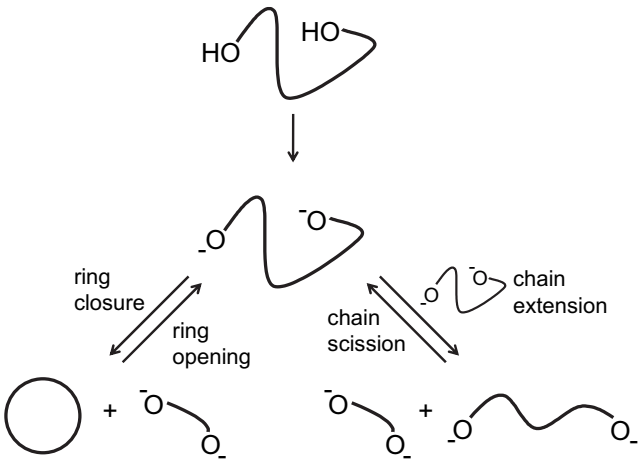

Fig. 1. Deprotonation of α,ω-dihydroxy-PDMS yields silanolate chain ends that initiate ring-chain equilibration. Dilute solution conditions promote the intramolecular process of ring closure, and concentrated conditions encourage the intermolecular processes of ring opening, chain scission and chain extension. Counter ions are not shown.

Cyclodepolymerization of PDMS has been reported in the literature. As early as 1946, Hunter et al. reported that "Cyclics in high yields are more readily prepared, however, by the depolymerization of dimethylsiloxane high polymers" [13]. They made this statement in reference to the production of cyclic dimethylsiloxanes by the hydrolysis of diethoxydimethylsilane or dichlorodimethylsilane monomers. Their method, which they called "destructive distillation", consisted of heating bulk PDMS fluid and cold trapping the volatiles. Following fractional distillation, cyclic $[(CH_3)_2SiO]_x$ was isolated with $x = 3$ up to $x = 8$, the relative amounts gradually decreasing with increasing ring size. While the method worked by simply heating bulk PDMS at atmospheric pressure to >350 °C, greater proportions of the larger rings were obtained by heating under vacuum to >230 °C in the presence of powdered sodium hydroxide. They noted that PDMS cycles larger than the octamer were probably broken down before volatilization could occur. Destructive distillation of bulk fluid has also been used to prepare cyclic oligomers with dimethylsiloxy and hydromethylsiloxy units, again with isolation of rings only up to the octamer [17]. Montaudo et al. treated high-molecular weight PDMS with 0.2% (w/w) NaOH at 250 °C for 2 h and showed using matrix-assisted laser desorption/ionization time-of-flight (MALDI-ToF) mass spectrometry that the sample consisted of both linear and cyclic PDMS [18]. Using MALDI-ToF, they were able to show that $[(CH_3)_2SiO]_x$ much larger than the octamer, at least up to $x = 34$, was prepared by this base-catalyzed cyclodepolymerization of bulk PDMS. Yields were not reported as their intention was not the development of a preparative route to cyclic PDMS.

Brunelle elegantly described the important concepts of kinetically controlled cyclodepolymerization in reference to their studies of metal-alkoxide-catalyzed depolymerization of poly(butylene terephthalate) [9]. He noted (i) dilute solutions favor intramolecular over intermolecular reactions, (ii) backbiting yields a cycle and a shorter linear chain, which can further backbite to yield another cycle, and (iii) initially the concentration of larger cyclics is greater than at the end of the reaction. This last point is key for the formation of rings larger than those dictated by equilibrium. If the reaction is allowed to proceed long enough, the cyclic distribution should be the same whether the starting material is low-molecular weight monomer or high-molecular weight linear polymer. By beginning with high-molecular weight linear polymers in dilute solution, the possibility exists for preparing high-molecular weight cyclic polymers by backbiting. Even though numbers of small cycles formed per unit time are always greater, larger cycles represent significantly more mass so that their yields are greater than with procedures that begin with monomers and build high-molecular weight through ring-chain equilibration [19]. This has been shown experimentally for cyclic aromatic disulfide oligomers: higher yields of the larger cycles are prepared by cyclodepolymerization of linear precursors as opposed to their conventional synthesis via oxidative-coupling polymerization of aromatic dithiol monomers [11].

Thus, while precedence exists in the literature for the preparation of cyclic PDMS by cyclodepolymerization of linear PDMS, at least in the bulk, this has not been explicitly described and compared to the ring-chain equilibration route. In this contribution we report that larger PDMS cycles may be prepared in greater yields by kinetically controlled cyclodepolymerization of linear PDMS in dilute solution, than by thermodynamically controlled ring-chain equilibration beginning with dimethylsiloxane monomer. Cyclic PDMS remains of interest for fundamental studies of topological effects on polymer physical properties [20], for the preparation of amphiphilic polyrotaxanes [21], and as complexing agents analogous to crown ethers [22].

2. Experimental section

2.1. Materials

All reagents were used as received. α,ω-dihydroxy-PDMS was purchased from Gelest (45–85 cSt, $M \sim 2000$–3500 g/mol, $M_n \sim 2.5$ kg/mol [6]; 700–800 cSt, $M \sim 18$ kg/mol). Sodium hydride (dry, 95%), 1-naphthyl isocyanate (98%), tetrahydrofuran (anhydrous, 99.9%), hexane, methanol and toluene (HPLC grade) were purchased from Sigma–Aldrich. Macroporous anionic-exchange resin AG MP-1 M (1 meq/mL, 0.7 g/mL, 100–200 mesh, chloride form) was purchased from Bio-Rad Laboratories and dried under vacuum prior to use.

2.2. Instrumentation

Samples for gel permeation chromatography (GPC) were prepared in a 1 wt% solution of toluene and filtered through a 0.45-μm nylon filter, with an eventual injection volume of 100 μL. GPC was conducted in toluene (1 mL/min) at 303 K on three Waters Styragel columns (5-μm beads: HR 1, 100 Å; HR 3, 1000 Å; HR 4, 10,000 Å) or (5-μm beads: HR 5; HR 1; HR 3) that were connected to a Waters 2690 separations module, 2487 dual-wavelength UV–Vis detector (set to 230 nm), and 2410 differential refractive index detector. The latter column set was employed when higher resolution was desired for species below 3 kg/mol. A calibration curve was computed by fitting a third-order polynomial to the log M versus retention time plot prepared from six polystyrene standards (1.26, 3.79, 13, 30.3, 65, 668 kg/mol). Universal calibration was employed using the following Mark–Houwink constants: $k_{PS} = 0.0075$ [(mL/g)(mol/g)^a], $a_{PS} = 0.75$ [23], $k_{PDMS} = 0.0042$ [(mL/g)(mol/g)^a], and $a_{PDMS} = 0.83$ [1]. For cyclic PDMS, k_{PDMS} is the same and $a_{cPDMS} = 0.77$, reflecting the smaller size in solution for a given molecular weight [1].

MALDI-ToF mass spectrometry was carried out on a Micromass TofSpec 2E operated in linear mode with α-cyanohydroxycinnamic acid as matrix. Ambient sodium ions or NaI were used for ionization and spectra were smoothed to reduce noise levels. IsoPro 3.0 was used to simulate isotopic distributions of peak assignments. ^{1}H, ^{13}C and ^{29}Si NMR spectra were measured on a Bruker AMX 400 or DRX 500 in chloroform-*d*.

2.3. Synthesis

Glassware was dried at 120 °C overnight. Round-bottom flasks with stir bars were sealed with rubber septa and cooled while evacuating and then backfilling with dry N_2. In a 250-mL flask with magnetic stir bar under positive nitrogen pressure, a septum was removed and sodium hydride (>2 eq based on M_n of α,ω-dihydroxy-PDMS, cf. Table 1) was transferred into the flask using a spatula. The flask was then evacuated and THF (200 mL) was charged by cannula. After allowing a minimum amount of time for the sodium hydride to fully suspend and dissolve (typically ~5 min), α,ω-dihydroxy-PDMS was added with a syringe and the mixture was stirred. It is important that the PDMS concentration, which was 7.5–10 g/L, be below the critical concentration for overlap (c^*). This was estimated as $c^* = 1/kM^a$, where M, k and a are the molecular weight and Mark–Houwink constants, respectively, of the linear PDMS precursor.

Aliquots were extracted with a syringe at various times after addition of the PDMS. The aliquot was quenched with one of two different agents: an anion-exchange resin for extracting the residual linear species, or 1-naphthyl isocyanate (>2 eq based on number of PDMS chains, cf. Table 1) to label the linear species with a UV-absorbing group. After quenching, the reaction mixture was filtered and solvent removed by rotary evaporation. The crude product was dissolved in hexane, washed with distilled water (×2), dried over magnesium sulfate and filtered. The filtrate was then poured into cold methanol to precipitate a clear viscous oil; the resulting mixture was centrifuged, decanted and dried under high vacuum. Dissolution in hexane and precipitation into cold methanol was repeated until GPC revealed that all remaining naphthyl groups were attached to PDMS chains.

Linear α,ω-dihydroxy-PDMS. ^{1}H NMR ($CDCl_3$): δ −.02–.40 (m, CH_3SiCH_3), 2.53 (s, HOSi). ^{29}Si NMR ($CDCl_3$): δ −10.7 (s, HOSi), −20.5, −21.41, −22.02 (m, CH_3SiCH_3). ^{13}C NMR ($CDCl_3$): δ .88–.42, .082 (m, CH_3SiCH_3). IR: broad, 3100–3700 cm^{-1}.

Cyclic PDMS. ^{1}H NMR ($CDCl_3$): δ −.02–.40 (m, CH_3SiCH_3). ^{29}Si NMR ($CDCl_3$): δ −22.02 (m, CH_3SiCH_3).

Linear PDMS with naphthyl end groups. ^{1}H NMR ($CDCl_3$): δ −.02–.40 (m, CH_3SiCH_3), 8.01–7.32 (7H, m, naphthyl end group).

2.4. Simulation algorithm

A kinetic Monte Carlo scheme was developed to examine the time evolution of topology, molecular weight distribution, and cyclic yield for unimolecular ring closure. The simulation was designed to approximate base-catalyzed cyclodepolymerization of α,ω-dihydroxy-PDMS in dilute solution. This was accomplished by creating a sample of linear precursor chains that were allowed to backbite and yield cycles (D_4 or larger) plus a smaller linear byproduct. The linear precursors and byproducts were allowed to backbite until a linear byproduct containing ≤4 siloxane units was created, after which it was removed from the simulation. Only intramolecular ring closure reactions were allowed and only one end group was allowed to backbite. A given linear species was allowed to backbite at any point along its chain, with the location governed by the relative rates of cycle formation of a given size. The relative rates of cycle formation were calculated from literature data on end-to-end cyclization rates determined from fluorescence studies of linear PDMS of various molecular weights end-labeled with pyrene groups [24]:

$$\log\langle f_x\rangle = -1.25\log(x) + 9.54 \quad (1)$$

where f_x represents the end-to-end cyclization frequency or rate (s^{-1}) of a linear chain with x repeat units. These cyclization rates were utilized in the Monte Carlo scheme as a weighting factor for random generation of the cyclic products by intramolecular ring closure. The likelihood that a ring with x repeat units, D_x, will be formed from a chain with y repeat units is directly related to the relative frequency of the end-to-end cyclization rates, $\delta(x) = f_x/f_y$, where x and $y \geq 4$.

The linear PDMS precursor was created with a user-defined number-average molecular weight (M_n) and polydispersity (PD) characterized by a Gaussian molecular weight distribution:

$$N_y = \frac{1}{\sigma\sqrt{2\pi}} \times \exp\left(-\left[\frac{(y^*74 + 18) - M_n}{2\sigma}\right]^2 \right) \quad (2)$$

where N_y is the number of chains in the distribution with y repeat units, σ is the width of the distribution, the repeat-unit molecular weight is 74, and the molecular weight due to end groups in α,ω-dihydroxy-PDMS is 18 g/mol. The width of the distribution is given by $\sigma = M_n \times (PD - 1)^{1/2}$ and the total number of chains in a sample is N. For the simulations reported here, N = 28,000. A Matlab code was written to generate a sample of linear precursor and then allow the entire population to form cycles according to the kinetic Monte Carlo scheme described above. After each cyclization event, the program keeps track of the resulting linear and cyclic distributions over the entire population so that the kinetic evolution of topology, molecular weight distribution, and cyclic yield can be followed.

Cyclization of a linear polymer is accompanied by a decrease in its hydrodynamic volume; this is manifested experimentally as an increase in retention time by gel permeation chromatography (GPC). Retention times (RT) can be determined for a given molecular weight (M) by solving the following equation:

$$\log\left(kM^{1+a}\right) = c_1 + c_2(\mathrm{RT}) + c_3(\mathrm{RT})^2 + c_4(\mathrm{RT})^3 \quad (3)$$

in which k and a are the Mark–Houwink constants for cyclic or linear PDMS, and the coefficients c_1 through c_4 were taken from the actual calibration curve determined using low-polydispersity samples with known molecular weight. Theoretical GPC retention time shifts can be calculated by taking the difference in the computed RT of the simulated linear PDMS precursor sample and its cyclic product derived using the Monte Carlo scheme.

Table 1
Reagent amounts used for cyclodepolymerization of α,ω-dihydroxy-PDMS in 0.2 L THF.

	α,ω-Dihydroxy-PDMS (g)	NaH (mg)	1-Napthyl isocyanate (mg)[a]
2.5 kg/mol	2	40	340
18 kg/mol	1.49	10	50

[a] Used only to label residual linear species with UV-absorbing group for dual-detector GPC analysis.

3. Results and discussion

3.1. Characterization of cyclic product mixtures with GPC and MALDI-ToF

A time-resolved study was performed using gel permeation chromatography (GPC) to track the formation of cyclic PDMS and general evolution of the product mixture upon deprotonation of α,ω-dihydroxy-PDMS in dilute solution. Fig. 2 shows the GPC traces of the resin-quenched product after addition of a 2.5 kg/mol or 18 kg/mol linear precursor to a NaH/THF solution. In general, the products from both molecular weights exhibit an increase in retention time as a function of time after addition, which is due to a reduction in

hydrodynamic volume caused by cyclization, a reduction in molecular weight, or both. To make any substantial conclusion about whether cyclization occurs, these GPC data were complemented with IR, NMR and MALDI-ToF mass spectra.

For the low-molecular weight precursor (2.5 kg/mol), IR and NMR data indicate a complete disappearance of silanol end groups after just 5 min. This is consistent with a MALDI-ToF mass spectrum of the same sample that contains a distribution of peaks that, after subtraction of the ionizing species, are separated and evenly divisible by 74 amu, the mass of the PDMS repeat unit. Lastly, the gravimetric yield of the purified cyclic product collected at 5 min is ~78%. Since resin purification has been shown to effectively remove linear byproducts [6], and along with the retention time increase observed in Fig. 2, these results all point to the formation of cycles. Thus, cyclic PDMS was prepared rapidly in high yield by this base-catalyzed unimolecular ring closure of deprotonated α,ω-dihydroxy-PDMS in dilute solution.

The rapid formation of cycles should not be surprising considering that cyclization requires only one of the chain ends of the linear precursor to find its own backbone. Cyclization timescales have been reported from fluorescence studies of intramolecular excimer formation in linear PDMS end-labeled with pyrene groups [24,25]. For a PDMS chain with M_n = 6.6 kg/mol, the mean cyclization rate constant is 10^6 s^{-1}. This generally increases with decreasing molecular weight and is also higher for chain end cyclization with interior parts of the chain. This latter point is important as it is expected the deprotonated PDMS chain ends backbite at interior points of the chain to produce cycles that are smaller than those that would be prepared by end-to-end coupling. The slight broadening of the GPC peak for the 2.5 kg/mol sample at 5 min reflects the consequent change in the molecular weight distribution. As the reaction proceeds beyond 5 min, the GPC peak continues to broaden and becomes increasingly multimodal, signifying progression of the reactions shown in Fig. 1 and a general reduction in the average molecular weight of the product. After 3 h, the main GPC peak for the product derived from the 2.5 kg/mol precursor appears at ~26 min, and persists as the main peak even after an 18-h equilibration period. This retention time corresponds to a ring size of ~15 repeat units (~1100 g/mol), which is apparently a slightly preferred size in this size range as a plot of the molar cyclization constants versus PDMS ring size reveals a local "stability maximum" at D_{15} [2].

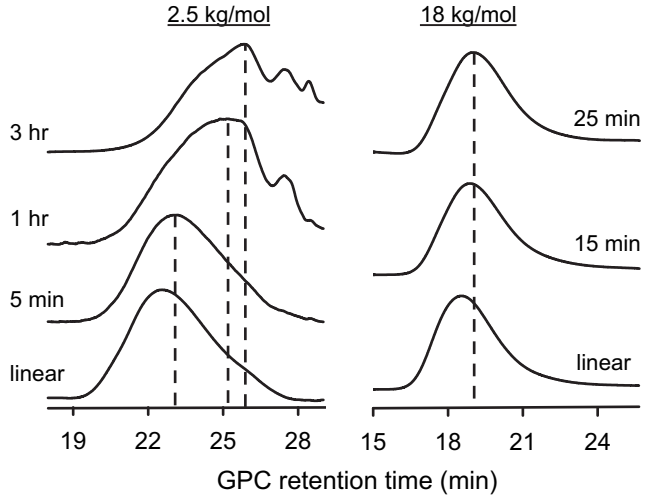

Fig. 2. GPC traces of linear α,ω-dihydroxy-PDMS and the product following its deprotonation in dilute solution and quenching with ion-exchange resin to remove charged linear species. Molecular weights at top refer to the linear precursor: M_n ~ 2.5 kg/mol (45–85 cSt) and M ~ 18 kg/mol (700–800 cSt). Times after addition of linear precursor to NaH/THF solution are indicated.

Fig. 2 reveals that, during depolymerization, the larger PDMS precursor also exhibits a shift toward longer GPC retention times. However, for high-molecular weight precursors with low concentrations of end groups, it can be difficult to determine whether the end groups have disappeared using NMR or IR spectroscopy. MALDI-ToF mass spectroscopy has proven useful in such instances. The MALDI-ToF mass spectrum of the resin-quenched product trapped 25 min after deprotonation of the 18-kg/mol linear precursor is shown in Fig. 3. It contains two sets of peaks separated by 74 amu, the mass of the PDMS repeat unit. The most intense set of peaks (i.e., major distribution), which includes the peaks marked (a) and (b) in Fig. 3, is due to sodium-cationized cyclic PDMS. The large peak at 3138 amu (a) is due to cyclic PDMS with 42 repeat units (D_{42}). Located 18 amu to the right of each peak of the major distribution, a low-intensity peak represents sodium-cationized linear PDMS with the same number of repeat units. This minor distribution, which includes the peak marked (c), is just above the noise level and remains constant in intensity throughout the mass range shown, while those due to cyclic PDMS decrease in relative intensity with increasing mass. These data clearly indicate that most of the product below about 5 kg/mol is cyclic PDMS.

The inset of Fig. 3 shows an expanded view of a pair of peaks along with the simulated spectra for a 65-repeat-unit PDMS cycle (o) and chain (□) cationized with Na^+, which confirm the assignments discussed above. Also shown is the simulated spectrum for a 65-repeat-unit linear PDMS cationized with H^+ (*x*), which is very close to the peak we assign to Na^+-cationized D_{65} (o). Since the matrix used is CHCA and ambient sodium is present, ionization could have occurred with H^+ and Na^+. Even though the peaks overlap, the best match between simulation and experimental data clearly confirms that the major peaks are due to cyclic PDMS.

For masses ≥~5500 amu, the cyclic and linear peak intensities are roughly equivalent indicating the resin is not as effective at removing higher molecular weight linear byproducts, and the efficiency of detecting cyclic PDMS relative to linear PDMS decreases with increasing mass. A resin with a given mesh size, or crosslink density, should exhibit reduced ion-exchange permeability and available surface area for absorbing higher molecular weight material. Ideal MALDI-ToF conditions (i.e., matrix, cationizing agent, etc.) are often not the same for different polymers. Linear PDMS contains polar end groups, which could facilitate ionization, while cyclic

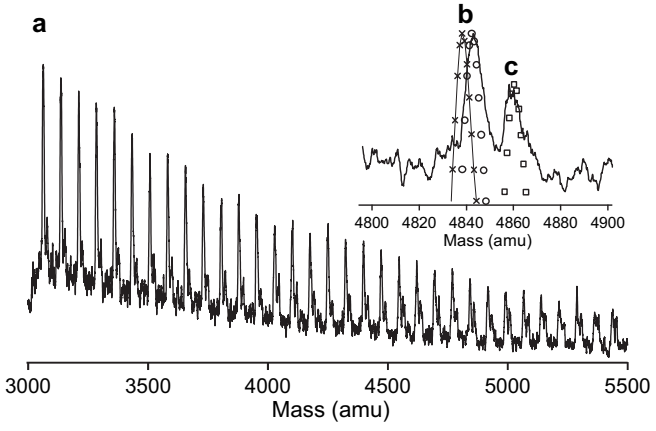

Fig. 3. MALDI-ToF mass spectrum of the product trapped 25 min after deprotonation of α,ω-dihydroxy-PDMS (M_n ~ 18 kg/mol, 700–800 cSt). (a) 3138 amu = Na^+/cyclic PDMS of 42 repeat units, (b) 4843 amu = Na^+/cyclic PDMS of 65 repeat units, (c) 4861 amu = Na^+/linear PDMS of 65 repeat units. The inset shows an expanded view to illustrate the spectral distribution due to isotope combinations. The symbols represent simulated spectra for a 65-repeat-unit PDMS: *x* = H^+/linear PDMS, o = Na^+/cyclic PDMS, □ = Na^+/linear PDMS.

PDMS does not. Furthermore, it is well documented that MALDI-ToF discriminates against high-molecular weight species in polydisperse samples, an effect attributed to detector saturation with the low-molecular weight species [26]. As shown with GPC (cf. Fig. 2) and supported with simulations to be presented shortly, base-catalyzed depolymerization of PDMS leads to increased polydispersity by extending the molecular weight distribution toward lower molecular weights. Thus, MALDI-ToF spectra were not analyzed quantitatively in these studies.

To quantitatively examine the product mixture from the base-catalyzed cyclodepolymerization of the high-molecular weight linear precursor, a chromatographic method was developed to distinguish the linear PDMS from the total product mixture. Following deprotonation of the hydroxyl end groups to allow backbiting ring closure with formation of linear byproducts, the reaction was quenched with 1-naphthyl isocyanate (NI) (see Fig. 4). This makes the linear species UV-active (specific absorptivity, $\alpha_{NI} \gg \alpha_{PDMS}$) and therefore separately detectable with GPC using a UV detector. The entire PDMS product is detected using a differential refractive index (RI) detector. Thus, GPC with a UV and RI detector in series could be used to measure both the linear PDMS content and molecular weight of a product containing cyclic and linear PDMS. The total integrated intensity output (I) from each detector can be written:

$$I_{RI} = K_{RI} \sum N_x^{L+C} M_x^{L+C} \tag{4}$$

$$I_{UV} = K_{UV} \sum N_x^{EG} \tag{5}$$

where K_{RI} and K_{UV} are the detector and sample constants, $\sum N_x^{L+C} M_x^{L+C}$ is the total mass of cyclic (C) and linear (L) species (i.e., total mass of repeat units), and $\sum N_x^{EG}$ is the total number of UV-active end groups (EG). The constant K_{RI} includes the specific refractive index increment which is assumed here to be equivalent for cyclic and linear species. The constant K_{UV} includes the specific absorptivity for the end groups which should be independent of molecular weight. Using a low-molecular weight reference sample, the molar ratio of repeat units to end groups can be determined from NMR spectroscopy:

$$\text{molar ratio} = \frac{1/M^{RU} \sum N_x^{L+C} M_x^{L+C}}{\sum N_x^{EG}} \tag{6}$$

where M^{RU} is the molecular weight of a repeat unit. Multiplying the NMR-determined molar ratio by M^{RU} provides the ratio of repeat units to end groups determined by GPC, which can be used with equations (4) and (5) and the GPC chromatogram of the same reference material to determine the constants K_{RI}/K_{UV}. Now a sample with an unknown cyclic/linear ratio can be measured with GPC and the K_{RI}/K_{UV} constants used to determine the ratio of repeat units to end groups. By substituting $\sum N_x^{EG} = 2 \sum N_x^L$ and using the GPC calibration curve to determine M_i^L for a given retention time, $\sum N_x^L M_x^L$ can be calculated. The cyclic yield is then

$$\text{cyclic yield} = \frac{\sum N_x^{L+C} M_x^{L+C} - \sum N_x^L M_x^L}{\sum N_x^{L+C} M_x^{L+C}} \tag{7}$$

Note that this dual-detector GPC technique allows deconvolution of the cyclic and linear molecular weight distributions. This can not be accomplished by any other method except MALDI-ToF mass spectrometry, which could not be successfully employed for quantitative measurements on our PDMS mixtures.

The 2.5-kg/mol PDMS was cyclodepolymerized for a short time and quenched with a large excess of 1-naphthyl isocyanate (NI) to prepare a reference sample in which the ratio of repeat units to end groups was determined by NMR spectroscopy. The 18-kg/mol precursor was then cyclodepolymerized for 2 min and quenched with NI. Using the dual-detector GPC method described above, the cyclic yield was determined to be 88%, which is completely consistent with the value determined gravimetrically, 87%, after resin-quenching the reaction to remove charged linear species. However, we know the gravimetric yield is too high as MALDI-ToF revealed some linear species remain in the product (cf. Fig. 3). The cyclic yield determined by GPC might also be high as it depends on the complete and quantitative reaction of all linear end groups with NI. To help assess the magnitude of these over-estimations of cyclic yield, we turned to simulations.

3.2. Monte Carlo simulations of cyclodepolymerization

A kinetic Monte Carlo scheme was used to examine how the average molecular weights, molecular weight distributions, and cyclic yields evolved during cyclodepolymerization of α,ω-dihydroxy-PDMS in dilute solution. Table 2 shows some results as a function of cyclization step, and hence reaction time, for a linear PDMS with $M_n = 15$ kg/mol and polydispersity (PD) = 1.3, intended to approximate the 18-kg/mol linear precursor on which we have experimental data. Note that after just a single cyclization step, the yield of cyclics $[(CH_3)_2SiO]_x$ with $x > 12$ is 17%, which is already greater than the 13% yield reported for $x > 6$ cyclic siloxanes prepared by the traditional route of base-catalyzed equilibration of D_4 and D_5 in toluene [1]. The cyclic product after the first cyclization step has a number-average molecular weight of 3 kg/mol and a PD of 2.5; the average molecular weight decreases to 2 kg/mol but the PD remains nearly constant (slight increase to 2.6) by the end of the simulation. The end of the simulation occurs when all of the linear material that can form cycles has done so, as reflected by the continuous drop in the average molecular weight of the linear byproduct with increasing cyclization steps.

The increase in polydispersity from linear precursor to cyclic product is consistent with GPC (Fig. 2) and MALDI-ToF (Fig. 3) data. The most significant change with cyclization step observed in the data of Table 2 is the large increase in cyclic yield. From 17% after one cyclization, the % yield of large ($x > 12$) cyclics reaches 82% by the end of the simulation. This compares favorably with the gravimetric yield (87%) determined after resin-quenching the reaction to remove

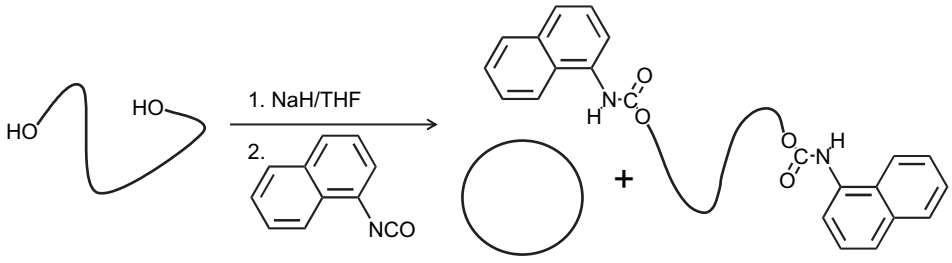

Fig. 4. Quenching the base-catalyzed cyclodepolymerization of α,ω-dihydroxy-PDMS with 1-naphthyl isocyanate gives linear byproducts with UV-active end groups.

Table 2
Simulated cyclodepolymerization of linear PDMS with M_n ~15 kg/mol, PD ~ 1.3.

Cyclization steps	Linear byproduct		Cyclic product		
	M_n (kg/mol)	PD	M_n (kg/mol)	PD	% yield, $x > 12$
1	11.4	1.4	3	2.5	17
2	9.6	1.5	2.8	2.5	30
3	8	1.6	2.7	2.5	42
5	5.7	1.8	2.4	2.6	59
10	2.5	2.7	2.2	2.6	79
20	0.4	2.8	2	2.6	82
50	–	–	2	2.6	82

charged linear species, and also with the yield determined using the dual-detector GPC method (88%) on a cyclic/linear mixture quenched with 1-naphthyl isocyanate to render the linear species UV-detectable. The similarities in cyclic yield (see Table 3 for a summary) suggest the following: the anion-exchange resin is effective at removing linear species, the dual-detector GPC method for analyzing cyclic/linear mixtures is valid, and cyclodepolymerization of linear PDMS under the conditions employed here is kinetically controlled.

The molecular weight data obtained from the simulation can be used with the universal GPC calibration curve to determine the theoretical retention time shift for the GPC chromatogram after any arbitrary number of cyclization steps (cf. Eq. (3)). The estimated shift to longer times should account for the reduction in molecular weight as reflected in the data of Table 2 and also the reduction in hydrodynamic volume due to cyclization. The retention time shift calculated for the sample after 5 cyclization steps was in reasonable agreement with that determined from the GPC data of the 18-kg/mol linear precursor and cyclic product after 2 min of base-catalyzed cyclodepolymerization in dilute solution.

The agreement between simulation and experiment sheds light on how base-catalyzed cyclodepolymerization can lead to higher yields for large cycles ($x > 12$) than those reported for base-catalyzed polymerization of D_4 and D_5. Beginning with a linear precursor, cycles of all sizes are formed by backbiting. A consequence of this is the production of cyclic material with a broad molecular weight distribution, even if the linear precursor is monodisperse. Large cycles form with reduced probability compared to small cycles, but take with them a disproportionately larger fraction of the mass from the linear feed source when they do form. A consequence of this is that longer linear precursors lead to higher yields of larger cycles. Fig. 5 shows the mass-based molecular weight distributions of cyclic product obtained by cyclodepolymerization of three different linear precursors: 2.5, 18 and 50 kg/mol. The yield of large cyclics ($x > 12$) increases with increasing precursor molecular weight from 69% to 82% to 92%. Experimental gravimetric yields for the 2.5 and 18-kg/mol linear precursors are 78% and 87%, respectively. Higher yields for longer linear precursors are consistent with the simulations (cf. Table 3).

Cyclic yield data can be represented as cyclic concentration, or molar cyclization constant K_x, versus number of repeat units x. For the thermodynamically controlled ring-chain equilibration of D_4, Brown and Slusarczuk found experimentally that $\log(K_x)$ scales with $\log(x)$ to the −2.86 power [2], which they reported as "the first experimental verification of the Jacobson–Stockmayer cyclization

Table 3
Cyclic yield ($x > 12$) from kinetically controlled cyclodepolymerization.

Linear precursor	Cyclic yield (%)		
	Gravimetric	GPC	Simulated
2.5 kg/mol	78	–	69
18 kg/mol	87	88	82

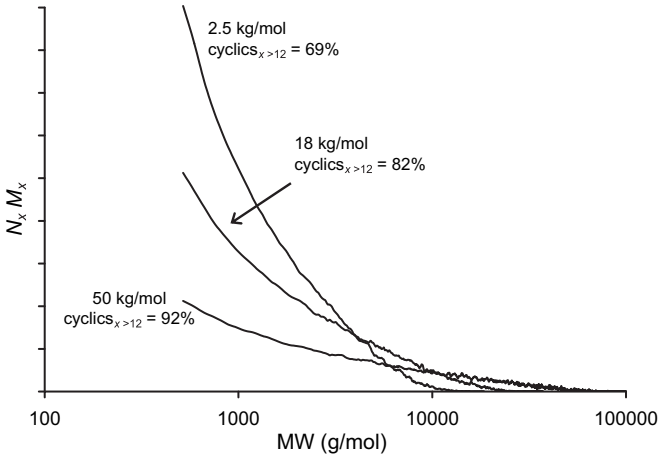

Fig. 5. Mass-based molecular weight distributions of cyclic product obtained by simulated cyclodepolymerization of linear PDMS of 2.5, 18, and 50 kg/mol (after 250 cyclization steps). Yield of cyclic PDMS with $x > 12$ is shown for each linear precursor. Each distribution represents same total mass.

theory" [27]. Beginning with Gaussian chain statistics, the theoretical scaling of $\log(K_x)$ with $\log(x)$ is −2.5 [27] for a ring-chain equilibration in which all of the reactions shown in Fig. 1 are allowed. By ignoring the reversible intermolecular reactions, the theoretical scaling of $\log(K_x)$ with $\log(x)$ is −1.5 since it is simply related to the probability of ring closure for a Gaussian chain [4,28]. Such kinetically controlled distributions have been observed experimentally and include the cationic polymerization/cyclization of D_3 [29]. Kinetic control leads to higher yields of larger cycles, but even higher yields are possible than those predicted theoretically. Fig. 6 compares the molecular weight distributions and yields of cyclic product calculated from theoretical cyclic distributions, both thermodynamically and kinetically controlled, with those obtained by Monte Carlo simulation of kinetically controlled cyclodepolymerization of an 18-kg/mol linear PDMS precursor. Cyclodepolymerization leads to 82% large cycles ($x > 12$) while kinetically controlled ring-chain polymerization leads to only 51%. Of course, the difference arises from the fact that the Monte Carlo simulation is based on a calculated scaling of −1.25 for log(cyclization rate) versus

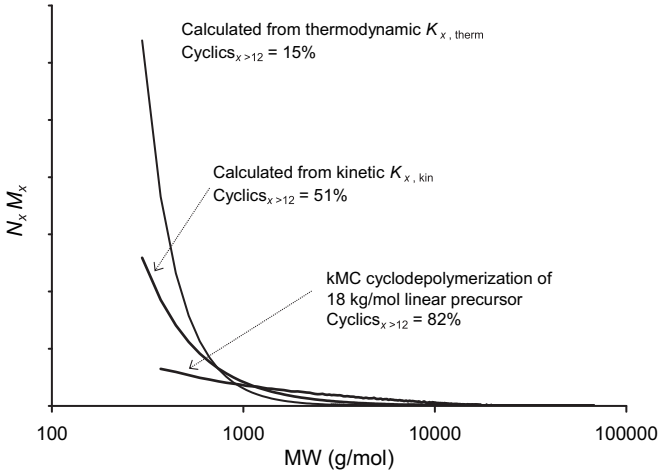

Fig. 6. Mass-based molecular weight distributions of cyclic product obtained by calculation from $\log(K_x)$ versus $\log(x)$ for thermodynamically and kinetically controlled ring-chain distributions, and kinetic Monte Carlo (kMC) simulation of cyclodepolymerization of 18-kg/mol linear PDMS. Each distribution represents same total mass.

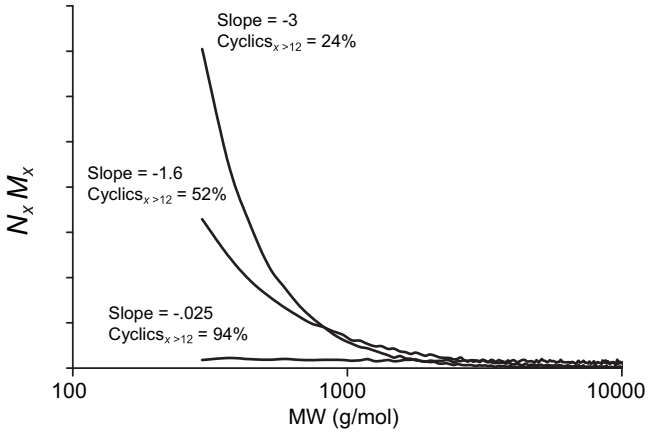

Fig. 7. Mass-based molecular weight distributions of cyclic product obtained by simulated cyclodepolymerization of 18-kg/mol linear PDMS using cyclization rates characterized by slopes of −3, −1.6, and −.025 in plots of log(f_x) versus log(x), where f_x is the cyclization rate for a chain with x repeat units. The experimental cyclization rate for PDMS is characterized by a slope of −1.25 (cf. Eq. (1)). Yield of cyclic PDMS with $x > 12$ is shown for each rate. Each distribution represents same total mass.

log(x) (cf. Eq. (1)), data that were taken from a literature report by Svirskaya et al. [24]. It should be noted that Svirskaya et al. did not report a fit to their experimental data but compared it to a theoretical line for which the slope is predicted to be −1.5 [24].

Thus, experimental adjustments that reduce the slope of cyclization rate versus size should lead to higher yields for larger cycles. This can be accomplished by adjusting solvent quality via solvent selection or temperature. In poor solvents, chains expand less rapidly with molecular weight than in good solvents due to excluded volume effects. As chains expand less rapidly their cyclization rate should fall less rapidly leading to a smaller slope in log–log plots of f_x versus x. An example can be observed in the literature on cyclization studies of end-labeled polystyrene (PS) [30,31]. The slope of cyclization rate versus chain size is smaller in cyclohexane, a poor solvent for PS, than in toluene, a good solvent. This should lead to higher yields of large PS cycles in cyclohexane than in toluene. Fig. 7 shows how the slope of cyclization rate versus size can affect the cyclic product molecular weight distribution. As the slope decreases, which means the relative cyclization rate for larger cycles increases, the relative amount of large cycles increases.

4. Conclusions

Cyclic PDMS (D_x) was prepared in high yield (>70% for $x > 12$) by kinetically controlled base-catalyzed cyclodepolymerization of linear α,ω-dihydroxy-PDMS in dilute solution. The yield of large cycles ($x > 12$) is higher for longer linear precursors. Yields obtained by this cyclodepolymerization route are much higher than those reported for the traditional route of base-catalyzed ring-chain equilibration of D_4 and D_5 (e.g., ~13%) [1]. In the traditional route, polymerization and cyclodepolymerization occur in competition, thereby limiting the production of large cycles. In cyclodepolymerization, the starting material is already high-molecular-weight, and even though the production of small cycles is always favored, the production of large cycles removes a disproportionately large amount of mass from the linear feed stock. Conducting the cyclodepolymerization in dilute solution allows kinetic control by suppressing intermolecular reactions (see Fig. 1) that would otherwise lead to an equilibrium ring-chain mixture.

A new GPC method was developed to quantitatively examine product mixtures of linear and cyclic polymers. The linear species were end-labeled with UV-absorbing groups and the product mixture analyzed with GPC using a differential refractive index and UV detector in series. A reference mixture containing low-molecular weight linear species was prepared and the ratio of total repeat units to end groups was determined by NMR spectroscopy. This reference mixture was measured with dual-detector GPC to establish the sample and instrument constants for the two detectors. These constants were then used to analyze the cyclic and linear content of unknown samples.

A kinetic Monte Carlo scheme was developed to simulate the evolution of topology and molecular weight distribution upon unimolecular ring closure. Resulting yields of large cycles ($x > 12$) were consistent with experimentally determined yields. The simulations were also consistent with experimental findings that higher yields of large cycles are obtained for longer linear precursors.

Acknowledgments

We gratefully acknowledge Bryan White for his contributions to this work. Partial stipend support was provided from the Georgia Tech GAANN program in Polymer Science and Engineering. MALDI-ToF spectra were collected by David Bostwick of Georgia Tech and Siming Wang of Georgia State University.

References

[1] Dodgson K, Semlyen JA. Polymer 1977;18:1265–8.
[2] Brown JF, Slusarczuk GMJ. J Am Chem Soc 1965;87(4):931–2.
[3] Semlyen JA, Wright PV. Polymer 1969;10:543–53.
[4] Wright PV, Beevers MS. Preparation of cyclic polysiloxanes. In: Semlyen JA, editor. Cyclic polymers. New York: Elsevier; 1986. p. 85–133.
[5] Dodgson K, Sympson D, Semlyen JA. Polymer 1978;19:1285–9.
[6] White BM, Watson PW, Barthelme EE, Beckham HW. Macromolecules 2002;35 (14):5345–8.
[7] Takahashi Y, Okajima S, Toshima K, Matsumura S. Macromolecular Biosci 2004;4:346–53.
[8] Okajima S, Kondo R, Toshima K, Matsumura S. Biomacromolecules 2003;4 (6):1514–9.
[9] Brunelle DJ. Cyclic oligomers of polycarbonates and polyesters. In: Semlyen JA, editor. Cyclic polymers. 2nd ed. Dordrecht, The Netherlands: Kluwer Academic; 2000. p. 185–228.
[10] Ben-Haida A, Hodge P, Colquhoun HM. Macromolecules 2005;38(3):722–9.
[11] Liang ZA, Meng YZ, Li L, Du XS, Hay AS. Macromolecules 2004;37 (16):5837–40.
[12] Kamau SD, Hodge P, Hall AJ, Dad S, Ben-Haida A. Polymer 2007;48:6808–22.
[13] Hunter MJ, Hyde JF, Warrick EL, Fletcher HJ. J Am Chem Soc 1946;68:667–72.
[14] Hall AJ, Hodge P. React Funct Polym 1999;41:133–9.
[15] Hodge P. React Funct Polym 2001;48:15–23.
[16] Höcker H. J Macromol Sci Pure Appl Chem 1993;A30(9–10):595–601.
[17] Chang P-S, Buese MA. Chem Mater 1993;5(7):983–8.
[18] Montaudo MS, Puglisi C, Samperi F, Montaudo G. Rapid Commun Mass Spectrom 1998;12:519–28.
[19] Ercolani G, Mandolini L, Mencarelli P. Macromolecules 1988;21(5):1241–6.
[20] Gagliardi S, Arrighi V, Ferguson R, Dagger AC, Semlyen JA, Higgins JS. J Chem Phys 2005;122:064904.
[21] Beckham HW, Nagapudi K, Girardeau T, Zhao T, Leisen J. Polym Prepr (Am Chem Soc Div Polym Chem) 2003;44(1):263–4.
[22] Decken A, Passmore J, Wang X. Angew Chem Int Ed 2006;45:2773–7.
[23] Oth J, Desreux V. Bull Soc Chim Belg 1954;63:285.
[24] Svirskaya P, Danhelka J, Redpath AEC, Winnik MA. Polymer 1983;24:319–22.
[25] Winnik MA. Spectroscopic studies of cyclization dynamics and equilibria. In: Semlyen JA, editor. Cyclic polymers. New York: Elsevier; 1986. p. 285–348.
[26] McEwen C, Jackson C, Larsen B. Int J Mass Spectrom Ion Processes 1997;160:387–94.
[27] Jacobson H, Stockmayer W. J Chem Phys 1950;18(12):1600–6.
[28] Goodman N, Morawetz H. J Polym Sci Part C 1970;31:177–92.
[29] Chojnowski J, Ścibiorek M, Kowalski J. Makromol Chem 1977;178:1351–66.
[30] Winnik MA. Acc Chem Res 1985;18:73–9.
[31] Winnik MA, Redpath T, Richards D. Macromolecules 1980;13(2):328–35.